Blocking cell extrusion prevents bronchoconstriction-induced airway epithelial damage and inflammation

Dustin C. Bagley#^†, Kristina Fox†, Polly F. Redd, Merry Joseph, Elena Ortiz-Zapater#, Maddy Parsons#, and Jody Rosenblatt#^*

#The Randall Centre for Cell & Molecular Biophysics, School of Basic & Medical Biosciences
^School of Cancer and Pharmaceutical Sciences, King's College London
†denotes equal contributions
*corresponding author, jody.rosenblatt@kcl.ac.uk

SUMMARY

Asthma is a common disease characterized by airway constriction, excess mucus, and inflammation. We previously showed that cell crowding drives steady-state epithelial cell extrusion and cell death. Using ex vivo lung slices, we show that excessive crowding from methacholine-induced bronchoconstriction causes extensive cell extrusion leading to destruction of the airway epithelial barrier. In live mice, bronchoconstriction-induced extrusion caused airway epithelia damage and inflammation in secondary and tertiary airways. In primary airways, bronchoconstriction triggered mucus secretion by a mechanism reminiscent of extrusion. Reversing bronchoconstriction with albuterol failed to ameliorate these symptoms, whereas inhibiting the stretch-activated calcium channel, Piezo1, prevented extrusion, inflammation, and mucus secretion. Our findings propose a new etiology for asthma where the mechanical crowding from bronchoconstriction causes so much extrusion that it compromises the barrier, triggering subsequent inflammation. Furthermore, inhibiting extrusion, potentially with gadolinium, an inexpensive Piezo1 inhibitor, may prevent the asthma inflammatory cycle.

KEYWORDS: asthma, extrusion, epithelial, airway, Piezo1, stretch-activated channel, mucus, airway smooth muscle, inflammation

INTRODUCTION

Greater than 339 million people suffer from asthma globally, with ~1000 dying from it daily. While both environmental and genetic factors contribute to asthma (Park and Tantisira, 2017), its etiology remains mysterious. Current therapies have greatly diminished many asthma symptoms (Olin and Wechsler, 2014) but cannot prevent future attacks. An asthma attack is characterized by bronchoconstriction, causing difficulty in breathing, wheezing, and increased airway mucus production. Depending on the severity of the attack, many asthma patients experience a post-attack inflammatory period with hypersensitivity to airway infections that can last from weeks to months and induce further attacks, triggering an inflammatory cycle (Holt and Sly, 2012).

Epithelia that line the airways provide a protective barrier for the lungs, acting as a first line of defense in innate immunity (Holgate, 2007; Holgate et al., 2009; Persson, 1996; Xiao et al., 2011). Central to providing a tight barrier to the outside world is maintaining constant epithelial cell densities as they turnover by cell division and death. We have identified a process essential for preserving epithelial cell number homeostasis called cell extrusion (Eisenhoffer et al., 2012; Rosenblatt et al., 2001). When an epithelial cell layer becomes too crowded, the stretch-activated calcium channel Piezo1 triggers live cells to extrude from the layer to preserve correct homeostatic densities (Eisenhoffer et al., 2012). To extrude, a cell produces the lipid Sphingosine 1-Phosphate to trigger a multicellular actomyosin ring that seamlessly squeezes the cell out while closing the gap that would have formed from the dying cell's exit (Gu et al., 2011). In this way, extrusion mechanically links the number of cells dying with those dividing to maintain constant cell densities and an intact barrier (Eisenhoffer et al., 2012; Eisenhoffer and Rosenblatt, 2013; Rosenblatt et al., 2001). Because mild physiological crowding normally causes cell death, we wondered if the bronchoconstriction of an asthma attack would cause so much crowding that it would trigger excess cell extrusion and compromise the airway epithelial barrier. If so, disrupting this protective barrier could lead to the inflammatory period and elevated susceptibility to viral and bacterial infection that typically follow an asthma attack (Castillo et al., 2017).

We found that bronchoconstriction causes excess extrusion and destruction of the airway epithelial barrier in ex vivo lung slices. Inducing bronchoconstriction in live mice similarly causes excessive extrusion, resulting in prolonged airway epithelial damage and inflammation 24 hours after an attack. Surprisingly, the crowding of bronchoconstriction also caused mucus secretion by a process that appeared similar to extrusion. Relaxing bronchoconstricted airways with albuterol, the current treatment, did not impede any of these downstream effects. However, inhibiting Piezo1 with gadolinium prevented extrusion, mucus secretion, and inflammation and can be used in combination with albuterol. Moreover, the mechanical basis for crowding, bronchoconstriction, that underlies all the asthma symptoms depends on amplification and restructuring of airway smooth muscle (ASM) surrounding bronchioles, suggesting an important, yet understudied role for smooth muscle in promoting inflammation.

RESULTS

Bronchoconstriction in ex vivo lung slices causes excess cell extrusion

To test if experimental bronchoconstriction could induce airway epithelial cell extrusion in a model where we could image events live, we treated ex vivo lung slices harvested from mice with methacholine (MCH) in culture (Gueders et al., 2009; Rosner et al., 2014; Struckmann et al., 2003). Methacholine is an agonist for acetylcholine receptors that triggers bronchoconstriction downstream of various asthma triggers, and is used clinically to test the severity of asthmatic airway hyper-responsiveness (Hopp et al., 1984). Live imaging of bronchioles confirmed that MCH treatment caused pronounced constriction of secondary and tertiary bronchioles within 5 minutes (Fig. 1 A, SMovie 1&2). Additionally, bronchoconstriction rapidly (within ~15 minutes) caused excess extrusion of epithelial cells lining the bronchioles. To quantify the number of extrusions, we counted the number of extrusions from lung slic-

es treated with increasing doses of MCH compared to untreated slices by fixing and immunostaining

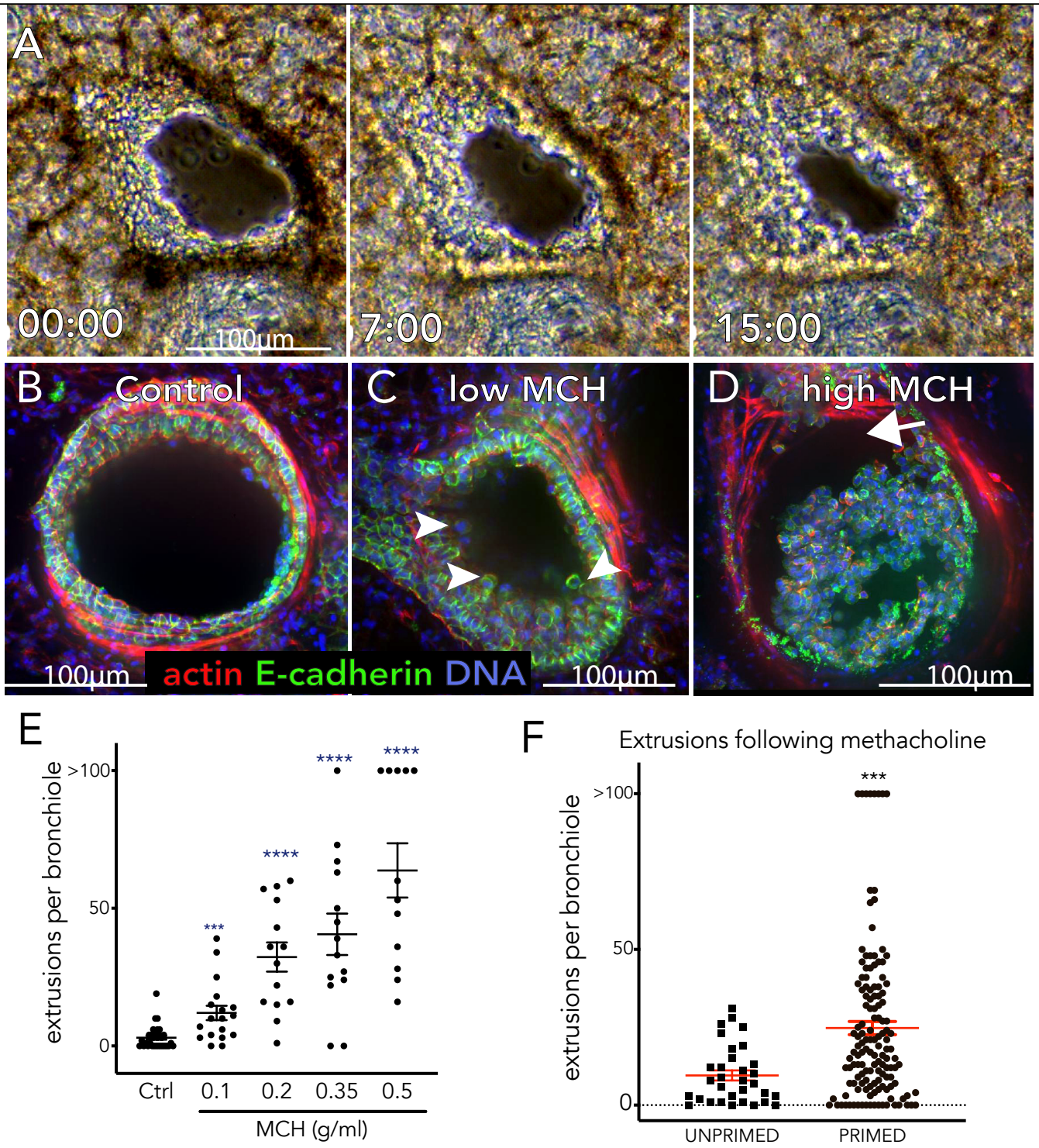

Fig. 1- Bronchoconstriction causes excessive extrusion in ex vivo lung slices. (A) Stills from constriction of a bronchiole, where 0.5 g/ml MCH is added at t=0:0 (minutes:seconds). Lung bronchioles treated for 30' with nothing (B) 0.2 g/ml (C) and 0.5 g/ml (D) MCH then fixed, and immunostained, with arrowheads pointing to individual extrusions and arrow, denuding or <100 extrusions on graph. (E) Number of extrusions seen per bronchiole with increasing concentrations of MCH, where 100 denotes all of the epithelia is gone or denuded, as seen in (D). (F) Only lung slices from immune-primed mice respond to methacholine. Where P****<0.0001 and P***<0.0005 for unpaired Mann-Whitney compared to control from over 10 mice each.

SFig. 1. Immune priming methods (A).Immune priming with OVA (A method) causes IgE expression by Elisa Assay (B), mRNA expression of cytokines IL-13 (C) and IL-4 (D), and MUC5A (E) by RT-PCR. Amplification of mucous in primary airways, as shown by PAS staining (F).

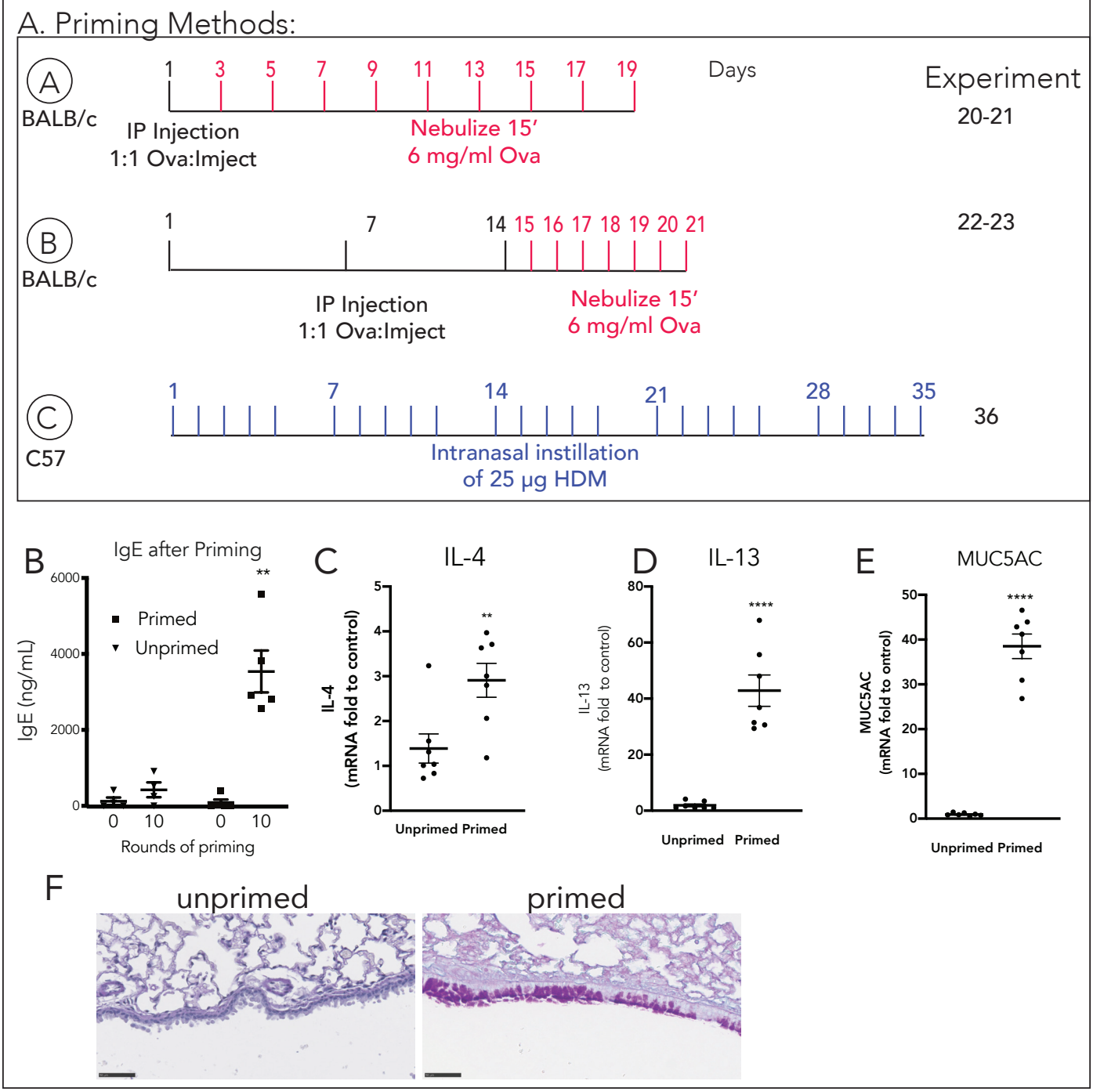

for epithelia with E-cadherin, airway smooth muscle (ASM) with phalloidin, and DNA with DAPI (Fig. 1 B-D). Generally, higher doses of MCH caused more cell extrusions from bronchioles, with highest doses (0.5g/ml) causing shedding or denuding of the entire epithelium, shown as <100 (Fig. 1 D&E).

Importantly, immune priming with ovalbumin (OVA) or house dust mite (HDM) is necessary for bronchoconstriction and extrusion in response to methacholine (Fig. 1F). To test if the extrusion we saw in response to methacholine-induced bronchoconstriction depended on the type of immune-priming,

we used several different published methods in two mouse strains (SFig. 1A). We found that all immune-priming methods induced pronounced bronchoconstriction and excess extrusion with methacholine treatment (see SFig. 1A and Methods for details). While OVA- (SMovie 1) and HDM-based (SMovie 2) priming caused similarly extensive extrusions in response to methacholine, for most experiments, we used the OVA protocols (see methods for details of each experiment). All protocols produced a characteristic Th2 inflammatory response found in most asthmatics, with increased inflammatory cytokines, mucus production, and venous IgE (SFig.1 B-E for OVA-priming, not shown for HDM). Thus, methacholine-induced bronchoconstriction of ex vivo slices from immune-primed mice causes airway epithelial cell extrusion and destruction.

Relaxing airways with albuterol does not impede extrusion

The short-acting ß2-adrenergic receptor agonist, albuterol, relaxes ASM and opens airways to facilitate breathing and could potentially prevent the excessive epithelial extrusion and denuding associated with bronchoconstriction. To investigate if reversing bronchoconstriction with albuterol prevents excess extrusion, we pretreated ex vivo lung slices with methacholine for 15 minutes and then treated with fresh methacholine with or without albuterol (schematic, SFig. 2A). Movies of these treatments show that albuterol relaxes airway constriction following methacholine treatment (Smovie 3). Surpris-

SFig. 2. Schematics for methods used to treat (A) *ex vivo* lung slices and (B) *in vivo* mice with methacholine.

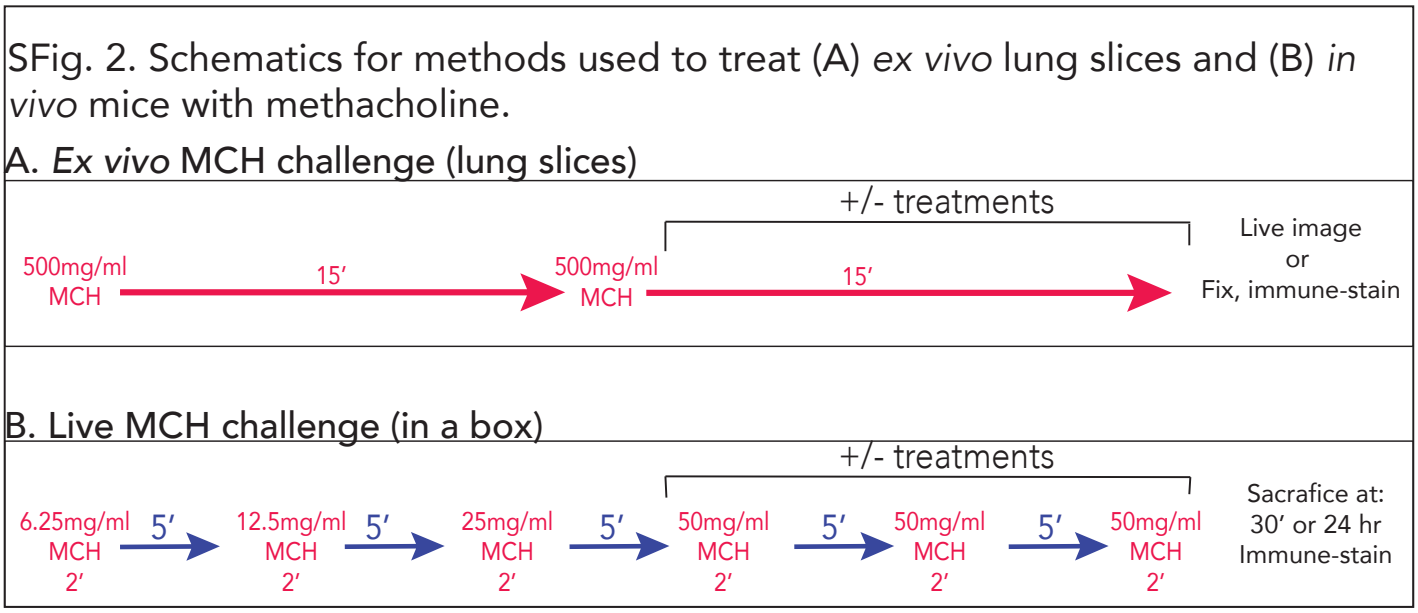

ingly, however, addition of albuterol to lung slices after bronchoconstriction did not prevent airway epithelial extrusion and destruction (Fig. 2 C-E). In fact, we frequently found that relaxation of the airways with albuterol produced more denuding by stripping epithelia from the smooth muscle as it relaxed, as seen in SMovie 3, Fig. 2A. Complete loss of airway epithelia in these cases could make its repair more difficult and chronic. For this reason, we instead quantified the percent denuding, rather than extrusions per bronchioles in our fixed immunostained lung sections. These data suggest that albuterol, the current treatment for bronchoconstriction, may still enable destruction of the airway lining

following an attack.

Gadolinium blocks extrusion caused by bronchoconstriction

Because crowding-induced extrusion requires the stretch activated channel, Piezo1 (Eisenhoffer et al., 2012), we tested if inhibiting Piezo1 could block the excessive extrusion resulting from the crowding

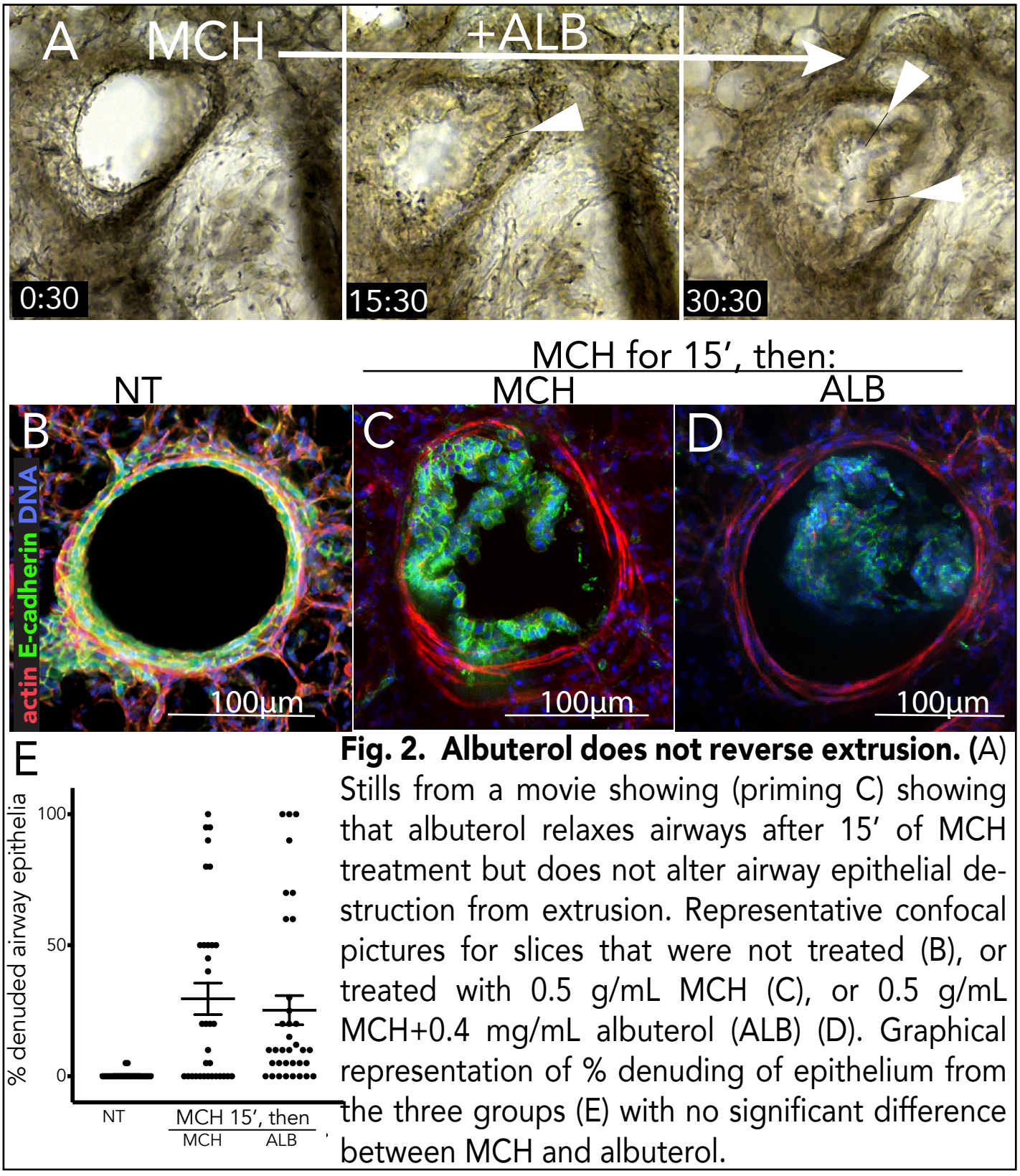

Fig. 2. Albuterol does not reverse extrusion. (A) Stills from a movie showing (priming C) showing that albuterol relaxes airways after 15′ of MCH treatment but does not alter airway epithelial destruction from extrusion. Representative confocal pictures for slices that were not treated (B), or treated with 0.5 g/mL MCH (C), or 0.5 g/mL MCH+0.4 mg/mL albuterol (ALB) (D). Graphical representation of % denuding of epithelium from the three groups (E) with no significant difference between MCH and albuterol.

of bronchoconstriction. Addition of the general stretch-activated channel inhibitor gadolinium hexahydrate chloride ($GdCl_3$) or the Piezo1 peptide inhibitor, GsMTx4 (Bae et al., 2011), dramatically reduced extrusion after bronchioles were constricted for 15 minutes with MCH (Fig. 3 A-D). Both treatments prevented the epithelial denuding seen with the highest MCH concentrations (Fig. 3 B-D, G). Since gadolinium works as well as GsMTx4 to block extrusion (Fig. 3F), but is less expensive and used clinically as an MRI contrast agent with limited toxicity, we used it in all subsequent studies. Importantly, albuterol did not impair the ability $GdCl_3$ to block epithelial extrusion/denuding following 15 minutes of MCH-induced bronchoconstriction (Fig. 3E, G, SMovie 4). Interestingly, airway epithelia appear to reattach to smooth muscle as it relaxes when gadolinium is added to albuterol (see SMovie 4). Thus, our ex vivo lung slice experiments show that gadolinium blocks the excessive extrusion and denuding of epithelia following bronchoconstriction in the presence or absence of albuterol, suggesting that it may prevent the inflammation that follows an asthma attack. To determine if preventing epithelial extrusion dampens inflammation, we developed an in vivo mouse assay.

Gadolinium blocks extrusion and damage of airway epithelia in live mice

To test if gadolinium inhibits extrusion in live mice as it did in our ex vivo slices, we induced bron-

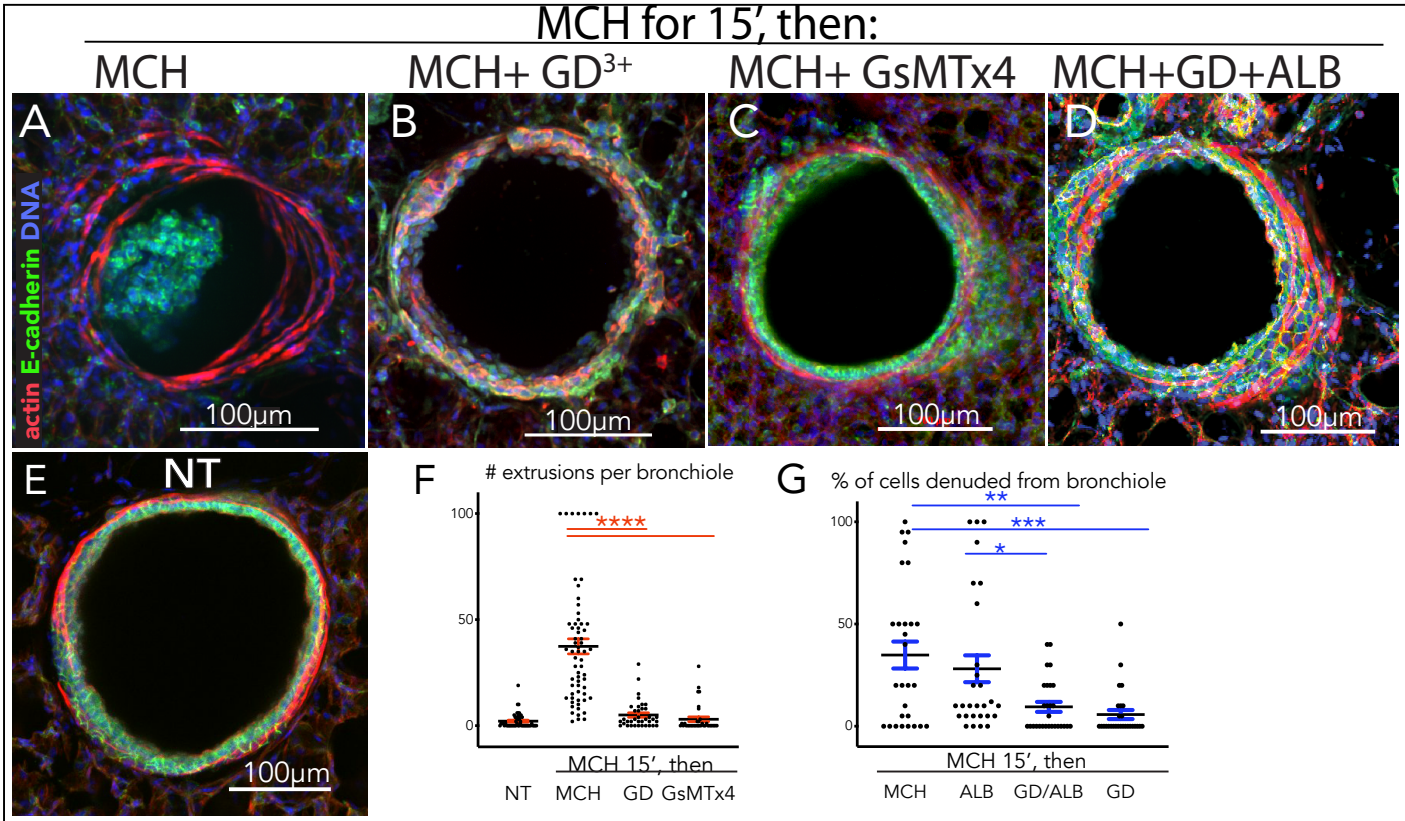

Fig. 3. Gadolinium blocks extrusion following MCH-induced bronchoconstriction. Representative pictures of bronchioles from *ex vivo* lung slices from OVA-primed mice (A method) treated with 500mg/ml MCH for 15', followed by MCH (A), MCH + $GdCl_3$ (B), MCH + GsMTx4 (C), or MCH + $GdCl_3$+ ALB (D), compared to no treatment (E). Graphical representations of extrusions per bronchiole (F) and % denuding (with ALB) (G), where each point represents a bronchiole from over 5 mice each and P***<0.0005 and P****<0.0001 of an upaired Mann-Whitney test. Denuding must be scored when ALB is present and there is no significant difference between MCH v. MCH/ALB or between GD v. GsMTx4 or GD v. GD/ALB.

choconstriction by nebulizing immune-primed mice with MCH with or without different inhibitors 15 minutes later. By treating immune-primed mice with increasing doses of MCH, we identified 50mg/ml (1/10 the concentration used in ex vivo experiments) as the lowest MCH dose that would trigger bronchoconstriction and extrusion (see schematic, SFig. 2B). To analyze the acute and inflammatory periods following bronchoconstriction, we sacrificed mice at 30 minutes or 24 hours after treatments and harvested their lungs for immunostaining and histological analysis. MCH treatment caused significant amounts of cell extrusion in live mice, compared to control-treated mice (Fig. 4A, B, I, J), albeit less than in our ex vivo studies. Importantly, MCH resulted in significantly damaged airway epithelia 24 hours later, scored by sheared epithelia that formed gaps in the layer or detachment of the epithelium seen by hematoxylin and eosin (H&E)-staining (Fig. 4 F&J). As with ex vivo lung slices, we find that re-

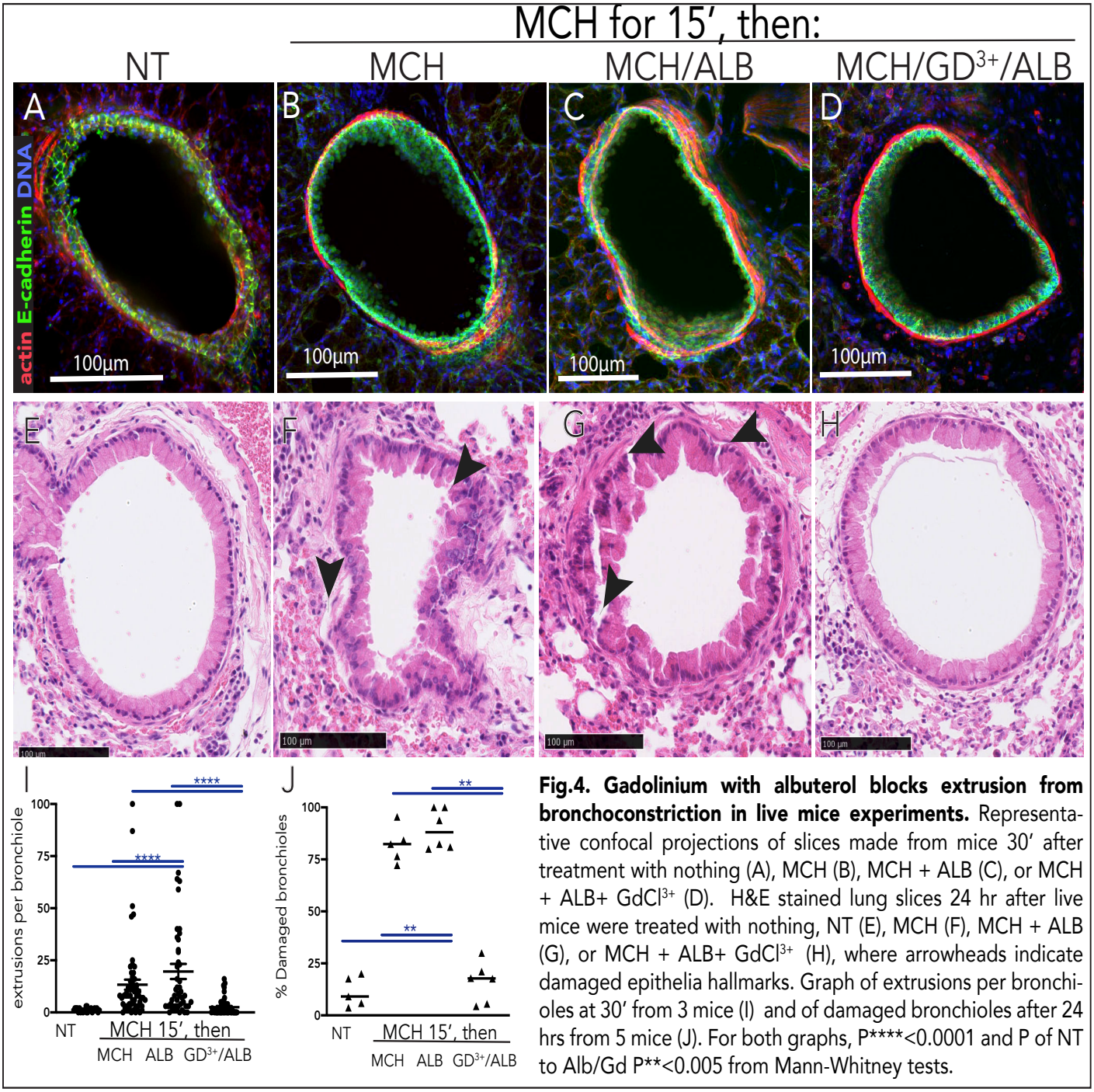

Fig.4. Gadolinium with albuterol blocks extrusion from bronchoconstriction in live mice experiments. Representative confocal projections of slices made from mice 30′ after treatment with nothing (A), MCH (B), MCH + ALB (C), or MCH + ALB+ $GdCl^{3+}$ (D). H&E stained lung slices 24 hr after live mice were treated with nothing, NT (E), MCH (F), MCH + ALB (G), or MCH + ALB+ $GdCl^{3+}$ (H), where arrowheads indicate damaged epithelia hallmarks. Graph of extrusions per bronchioles at 30′ from 3 mice (I) and of damaged bronchioles after 24 hrs from 5 mice (J). For both graphs, P****<0.0001 and P of NT to Alb/Gd P**<0.005 from Mann-Whitney tests.

laxing airway constriction with albuterol does not block extrusions nor does it prevent the bronchiolar damage 24 hours after MCH challenge (Fig. 4 C, G, I, J). However, addition of gadolinium to albuterol prevented extrusion and preserved airway epithelia at 24 hours (Fig. 4 D, H, I, and J). Because we find that albuterol does not impede the ability of gadolinium to block extrusion (Fig. 3 E, G, and data not shown) and is necessary for opening airways in patients, we used albuterol with gadolinium treatment in all our live mice studies to reduce total numbers of mice used. Thus, administering gadolinium even 15 minutes after methacholine-induced bronchoconstriction can prevent airway epithelial damage, suggesting that it might prevent the ensuing inflammatory period.

Gadolinium prevents inflammation after bronchoconstriction

Our live mouse experiments allowed us to assess if blocking airway epithelial extrusion and damage prevents inflammation following bronchoconstriction. H&E stained sections of lung slices from OVA-primed mice indicate that numerous immune cells accumulate at bronchioles 24 hours following methacholine-treatment, compared to control, untreated mice (Fig. 5 A, B&E, scored by classes of

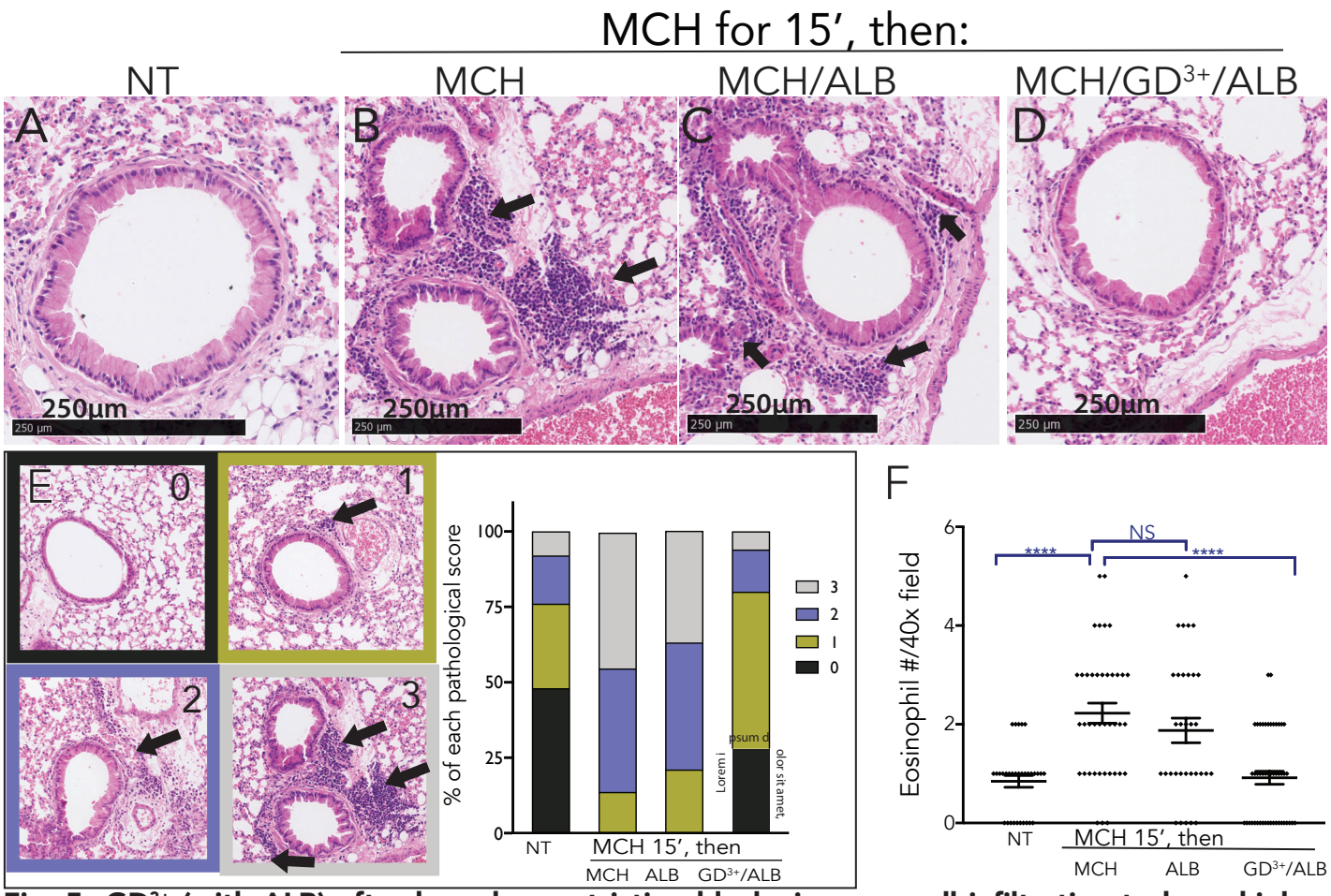

Fig. 5 GD³⁺ (with ALB) after bronchoconstriction blocks immune cell infiltration to bronchioles. Sample H&E sections from 24 hours after no treatment (A), or treatment with MCH for 5' followed by 30' treatment with MCH (B), MCH + ALB (C), or MCH + ALB + GD³⁺(D). Graph represents different pathological scores, as defined by colors/numbers, of immune cells recruited to bronchioles 24 hrs after treatment (E). In all pictures, arrows show immune cell infiltrates. Graph of eosinophiles from bronchiolar lavage after each treatment (F), where ****p<0.0001 from a Chi-squared test (E) and a Mann-Whitney test (F).

(1)<10, (2)<50, (3)>50). Additionally, bronchoalveolar lavage fluid (BALF) contained high numbers of eosinophils 24 hours after methacholine treatment, compared to controls (Fig. 5 F). While treatment with albuterol after methacholine treatment did not significantly alter immune cell infiltration or eosinophil numbers within airways (Fig. 5 B&E), addition of gadolinium with albuterol after bronchoconstriction reduced both to levels seen in control bronchioles (Fig. 5 A, D-E). Thus, gadolinium treatment, administered 15 minutes after bronchoconstriction prevents the inflammation that typically follows this event.

Gadolinium blocks mucus secretion

While asthma typically has the greatest effect on secondary and tertiary airways, most asthma patients experience significant difficulties with excess mucus secretion within the primary airways. We found that immune priming with ovalbumin caused increased mucus secretion, as measured by Muc5A qRT-PCR and amplified secretory cells, staining purple with Periodic Acid Schiff (PAS) staining of primary airways (SFig. 1E&F). We did not notice significant amounts of cell extrusions in primary airways following methacholine treatment, likely due to these airways experiencing comparatively less crowding than the smaller secondary and tertiary airways. However, histology with PAS staining indicated that MCH caused mucous cells to secrete excess mucus by a mechanism reminiscent of extrusion, where large globules of mucus were pinched out apically from cells (Fig. 6B, C, &E, arrowheads). Relaxing airway constriction with albuterol did not alleviate mucus secretion (Fig. 6B, C, &E). Surprisingly,

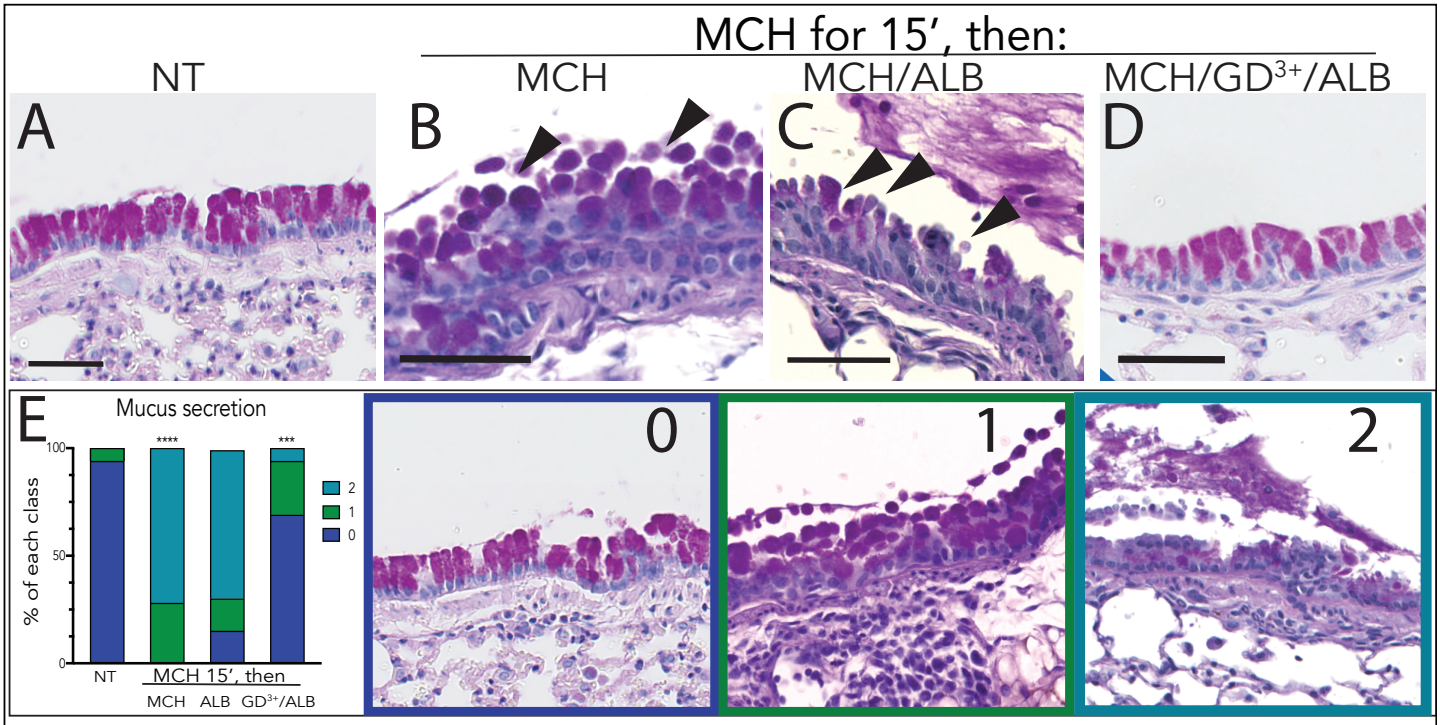

Fig. 6. Gadolinium blocks mucus secretion from large airways in live mice experiments. Representative PAS slices from primed mice (A) treated with MCH, followed by a high dose of MCH (B), MCH + ALB (C), or MCH + ALB+ $GdCl_{3+}$ (D). Scale bars=50μm. Arrowheads point to extrusion-like secretion of mucus. E, quantifications of mucus secretion by grades, where sample pictures of each grade are color coded, where p values of ****<0.0001 of a Chi-square test.

however, $GdCl_3$-treatment with albuterol dramatically reduced mucus secretion from primary airways, compared to albuterol alone or control-MCH treated mice (Fig. 6 D&E). While it is not clear why gadolinium treatment blocks mucus secretion, the similar extrusion morphology, and the fact that it results after mechanical constriction, suggests mucus secretion results from mechanical crowding of primary airways.

Immune-priming causes airway smooth muscle remodeling and amplification

Given that the mechanical crowding of bronchoconstriction is critical for excess extrusion, epithelial damage, inflammation, and mucus secretion, we investigated why immune priming causes mouse bronchioles to hyper-constrict in response to MCH whereas non-primed mice do not (Fig 1A, SMovies 1, 2 compared to SMovie 5). Others have found that ASM becomes amplified in bronchoconstrictive airways (Doeing and Solway, 2013) and is the critical factor for whether patients will bronchoconstrict in response to stimuli (Adams et al., 2016). However, it is not clear how ASM becomes altered to make airways hyper-responsive to MCH treatment. To examine morphological changes in ASM after immune priming, we imaged airway smooth muscle (ASM), labeled with phalloidin by confocal projection. While immune-priming amplifies ASM, it also alters its architecture. We found that bands of smooth muscle were not necessarily thicker but were instead more aligned in closer parallel bundles with few to no gaps, compared to unprimed ASM (Fig. 7 A-C). Because smooth muscle lacks sarcomeres (Herrera et al., 2005), the ASM remodeling into closer, longer bundles could cause airways to hyper-constrict when treated with MCH. By contrast, the lattice-like configuration of unprimed ASM may obstruct

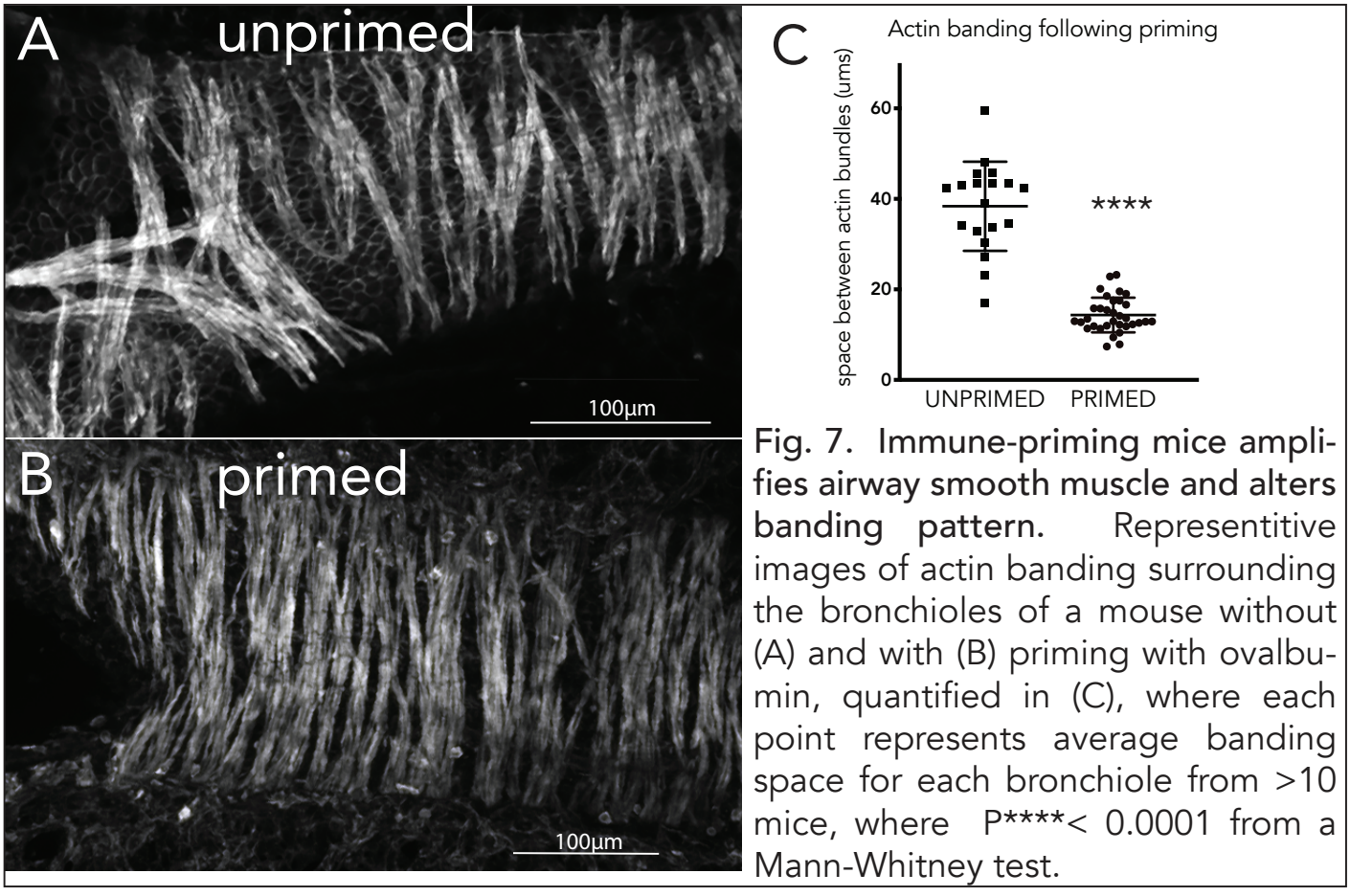

Fig. 7. Immune-priming mice amplifies airway smooth muscle and alters banding pattern. Representitive images of actin banding surrounding the bronchioles of a mouse without (A) and with (B) priming with ovalbumin, quantified in (C), where each point represents average banding space for each bronchiole from >10 mice, where P****< 0.0001 from a Mann-Whitney test.

excess contraction. Thus, the excess extrusion that causes inflammation following bronchoconstriction stems from uncontrolled constriction that likely depends on ASM alterations.

DISCUSSION

Here, we present a new etiology for asthma. Whereas most asthma studies have focused on the inflammatory signaling associated with asthma, our work has found a new role for the mechanics of bronchoconstriction causing most asthma symptoms. We found that bronchoconstriction causes excessive airway epithelial crowding, which causes so much cell extrusion that it destroys the barrier, resulting in inflammation (Graphical Abstract). Because epithelia act as the first line of defense against pathogens and toxins, epithelial barrier disruption could also cause infection hypersensitivity, until the airway epithelium repairs. Infections and inflammation could then lead to more bronchoconstrictive attacks, triggering the asthma inflammatory cycle (Yamaya, 2012). Moreover, constriction of primary airways causes mucus secretion using a mechanism like extrusion. We demonstrate that blocking extrusion following a bronchoconstrictive event preserves epithelial integrity, which dramatically dampens the immune response (Graphical Abstract). It also blocks mucus secretion from the primary airways, suggesting mechanical crowding controls mucus secretion using an extrusion-like mechanism. Importantly, albuterol treatment, standardly used by asthma patients to relax airways and breathe, does not prevent airway epithelia destruction, mucus secretion, or inflammation following an asthma attack. Our

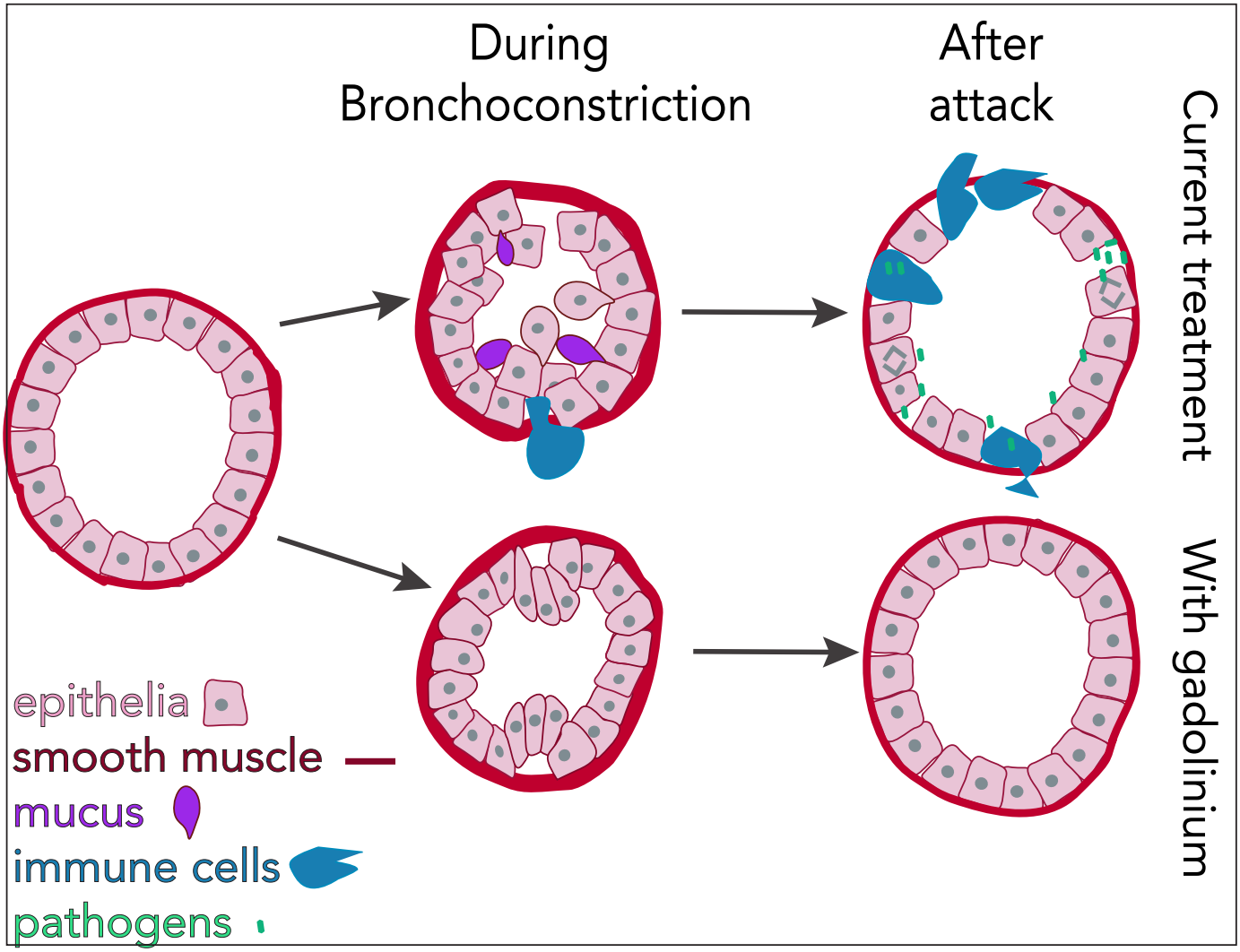

findings demonstrate that inhibiting extrusion can block not only inflammation and mucus secretion linked to asthma attacks but could potentially even prevent future attacks.

Importance of the epithelial barrier

Our findings highlight the importance of maintaining an intact airway epithelial barrier for preventing asthmatic inflammation. Others have noted the importance for airway epithelia in asthma (for instance, (Holgate, 2011; Tam et al., 2011)); here, we find that damage to this barrier results directly from the bronchoconstriction that defines an attack. This discovery stemmed from our previous findings that extrusion activated by ~1.6-fold crowding triggers most epithelial cell death during normal steady state turnover (Eisenhoffer et al., 2012). Our work suggests that an asthma attack leads to pathological levels of crowding and extrusion that destroys the barrier, causing inflammation. In addition to extrusion, we find that with very high crowding, entire sheets of epithelia delaminate into the airways. While it is not clear if this delamination occurs via an extrusion-like mechanism, the finding that gadolinium can block both extrusion and denuding suggests it shares similar signaling to extrusion. Our findings are consistent with human asthmatic airway biopsies that show 'fragile' airway epithelia with significant airway epithelial sloughing (Davies, 2009; Goldie et al., 1988; Hamilton et al., 2001).

It is noteworthy that triggers other than crowding that can cause cell extrusion (Andrade and Rosenblatt, 2011; Gu and Rosenblatt, 2012; Rosenblatt et al., 2001) could also cause barrier defects if overactivated. For instance, several viruses and bacteria can trigger excess extrusion that could similarly compromise the barrier (Deng et al., 2017; Liesman et al., 2014; Quantius et al., 2016). While Piezo1 activates cell extrusion via calcium upon crowding, TRPA1 and TRPV1 channels can activate calcium in response to particulate matter in pollution (Deering-Rice et al., 2015; Deering-Rice et al., 2016), suggesting that particulate matter and irritants might also trigger excess extrusion and inflammation. Interestingly, individuals with activating mutations in either TRP channel have poorly managed asthma (Deering-Rice et al., 2015; Deering-Rice et al., 2016). While these possibilities need further investigation, understanding that excess extrusion could cause airway epithelial damage and inflammation could improve our understanding of other triggers that could elicit inflammation and potentially future asthma attacks.

Use of gadolinium for asthma

Our findings that bronchoconstriction causes excessive extrusion led to a simple potential treatment—gadolinium. Treatment at the time of constriction or when applied even fifteen minutes after bronchoconstriction blocks most of the extrusion in methacholine-constricted airways. While albuterol on its own did not block airway epithelial damage, inflammation, and bulk secretion of mucus, it is still effective for relaxing airways, critical to breathing. Therefore, in our live mice studies we used albuterol with gadolinium to ensure that albuterol did not impede gadolinium. As with any compound, gadolinium has known toxicities and long-term use can affect renal function (Rogosnitzky and Branch, 2016). It is not known if renal toxicity results from gadolinium accumulation in the kidney or whether it affects cilia function, since it may inhibit TRPV4, which promotes ciliary beating through calcium (Lorenzo et

al., 2008). Thus, it will be important to determine the extent to which gadolinium might impair cilia or other function in primary airways before implementing it in humans.

However, gadolinium has many advantages to recommend its use as an asthma treatment. First, it is used frequently in a chelated form as a contrast agent for magnetic resonance imaging (MRI), suggesting that it may be well-tolerated in limited doses. Inhalation of gadolinium may prevent the systemic accumulation, associated with systemic injection. While airway inhalation of gadolinium has been studied (Bianchi et al., 2014), its long-term effects still need to be investigated. Second, since gadolinium is a non-specific stretch-activated channel inhibitor, it might prevent extrusion in response to pollution by blocking TRPA1 and TRPV1 channels, as mentioned above. This offers an advantage over more specific Piezo1 inhibitors like GsMTx4, which may more specifically prevent airway epithelial destruction from only bronchoconstriction. Currently, GsMTx4 is less studied, and may be more toxic than gadolinium, and expensive. However, it may act as a good basis for designing new ways to reversibly inhibit extrusion, should gadolinium prove toxic to airways. Finally, gadolinium could be implemented widely and rapidly, since it is already been in use for over 30 years. The fact that gadolinium is inexpensive is also important, given that asthma disproportionately affects lower income populations (Louisias and Phipatanakul, 2017; Pacheco et al., 2014).

Mechanically-induced mucus secretion

While primary airways experienced less crowding than secondary and tertiary airways during bronchoconstriction, we found that it experienced enough crowding to cause secretion of mucus. The fact that gadolinium, a stretch-activated channel inhibitor could also inhibit mucus secretion, suggests a new mechanical crowding role for mucus secretion, in addition to inflammation. It is not clear why crowding elicits mucus secretion in primary airways. One possibility is that mechanical pressure could directly squeeze it out. Alternatively, crowding could elicit calcium currents through Piezo1 or other channels that trigger mucus secretion. Indeed, previous work has shown that calcium ionophore is sufficient to elicit mucus secretion from canine tracheal explants (Barbieri et al., 1984) and that can calcium control regulated mucus secretion (Davis and Dickey, 2008). Additionally, both calcium and biophysical mechanisms may operate together. Our data suggest that crowding may act as the trigger for calcium-induced mucus secretion. More importantly, gadolinium treatment can impede the excess mucus associated with bronchoconstriction, which is a significant problem for most asthma sufferers. It may also suggest alternative etiologies for the excessive mucus suffered by cystic fibrosis patients.

Airway smooth muscle remodeling

A defining characteristic of asthmatics is amplification of airway smooth muscle (ASM) (Doeing and Solway, 2013). Along with launching an IgE response, immune priming mice caused ASM amplification and remodeling, which was predictive of whether bronchioles were hyper-responsive to methacholine treatment in our studies. Importantly, recent studies using birefringence microscopy showed that asthma patients have amplified ASM whereas unaffected individuals do not (Adams et al., 2016). Thus, triggers that normally cause ASM contraction trigger bronchoconstriction in individuals with amplified, hyper-responsive ASM. Our findings that airway epithelial barrier destruction results from

mechanical bronchoconstriction highlight the importance of understanding how ASM remodels to become hyper-contractile. In contrast to skeletal muscle that has Z-bands at short intervals, which limit its contraction, smooth muscle has long actin bundles that can contract without restraint. While smooth muscle lining unprimed bronchioles has large gaps and is more lattice-like in its structure, the ASM in immune-primed mice lacks interval spacing and appears to be in longer parallel bundles. Thus, upon neuromuscular activation, actin and myosin in smooth muscle could contract continuously without constraint.

How does ASM remodel to cause bronchoconstriction in asthma patients? Work from other labs suggests that both biophysical remodeling and chemical signaling may contribute to hyper-responsive ASM. In healthy airways, involuntary deep inspirations that occur approximately every ten inspirations break up airway smooth muscle constriction (Bendixen et al., 1964; Golnabi et al., 2014). Yet, amplified ASM makes it more difficult to deeply inspire and detach contracting actomyosin motors (Krishnan et al., 2008), which could mechanically jam as they constrict over time, amplifying ASM (An and Fredberg, 2007; Krishnan et al., 2008; Trepat et al., 2007). Additionally, signals that normally preserve intact epithelia could become aberrant in asthma. After an asthma attack, epithelia will need to proliferate to repair the wounding caused by excessive extrusion. However, to prevent the barrier disruption during this repair interval, a short-term strategy may be to reduce the surface area the epithelia need to coat by contracting underlying stroma or smooth muscle. Sphingosine 1-Phosphate (S1P), a secreted lipid necessary for extrusion, could provide a good candidate signal for activating ASM contraction and amplification, since disrupting S1P abrogates airway hyper-responsiveness (Oyeniran et al., 2015; Price et al., 2013). Alternatively, intact epithelia secrete BPIFA1/SPLUNC1, an inhibitor of ASM contraction (Wu et al., 2017). In this way, loss of epithelia from extrusion or other damage could cause ASM to contract and reduce the surface area until the epithelia regenerates. In asthma, an intrinsic, beneficial response that normally preserves the barrier could lead to pathological long-term constriction, which could amplify smooth muscle. Thus, severe asthma attacks could promote more asthma attacks by promoting continuous airway constriction. If so, blocking airway epithelial destruction during an asthma attack could have the potential to prevent further attacks. As ASM constriction is the central cause of bronchoconstriction, how ASM is regulated in normal and asthmatic airways demands more research and understanding.

Our findings propose a new paradigm for asthma etiology. While most research has focused on asthma primarily as an inflammatory disease, our findings suggest that aberrant mechanics drive not only the life-threatening inability to breathe, but also the associated inflammation and mucus secretion. Further, the wound healing associated with an attack could promote future attacks. From understanding the root cause of these asthma symptoms, we may be able to implement an inexpensive, commonly used compound to prevent these symptoms, which could ultimately prevent future attacks. Moreover, excess smooth muscle constriction may underlie other inflammatory syndromes, especially those linked with cramping, such as irritable bowel syndrome, and endometriosis, yielding new approaches

to these unsolved medical problems.

MATERIALS AND METHODS

Animal models and immune-priming methods

BALB/c mice at six-eight weeks of age where immunogen-sensitized in three of the following ways, by adapting and optimizing several protocols (S Fig.1). For intraperitoneal injections, 8mg/mL albumin from chicken (OVA) (Sigma – A5503) was absorbed into an equal volume of Imject® Alum (Thermo Fisher Scientific – 77161) before 200 µl of priming solution was intraperitoneally (i.p.) injected into mice, as stated in protocol in SFig. 1. Mice were then challenged with aerosolized OVA (6mg/mL for 15min), as indicated in in SFig. 1 for each protocol. All experiments were done within 48hrs of the last OVA challenge. For the House Dust Mite (HDM) immune-sensitized protocol, 6-8 weeks females C57B/6J mice were anesthetized with isofluorane and administered 25 mg (total protein) of HDM (Citeq Biologics, Groningen, The Netherlands) in 25 ml of PBS intranasally 5 times per week for 5 weeks. Control mice received 25 ul of PBS. Analysis was performed 24 hours after the final challenge. We used mice primed as in (A) for Figs.1B-F, 2B-E, 3, 4 A-D, & 7, as in (B) for Figs. 1A, 4 E-H, J, 5, & 6., SMovie 1, and as in (C) for Fig. 2A and SMovies 2-5.

All animals were maintained under specific pathogen–free conditions and handled in accordance with the Institutional Committees on Animal Welfare of the UK Home Office Animals (Scientific Procedures) Act 1986. All animal experiments were approved by the Ethical Review Process Committee at King's College London and carried out under license from the Home Office, UK. All mice were humanely handled, according to an IACUC license 16-08007 from the University of Utah and a Program Project License to Jody Rosenblatt at King's College London.

Ex vivo lung slices

Ex vivo lung slices were obtained from mice, within 48hrs of their last OVA challenge, adapted from the protocol in ref (Akram et al., 2019)). Briefly, mice were humanely killed by CO_2 inhalation followed by cervical dislocation. The chest cavity was opened and the trachea carefully exposed, where a small incision was made to accommodate the insertion of a 20Gx1.25 in canula (SURFLO I.V. catheter). The lungs were inflated with 2% low melting agarose (Fisher – BP1360) prepared in HBSS+ (Gibco – 14025) before lungs, along with the heart and trachea, were excised, washed in PBS, and the lobes separated. Individual lobes were then embedded in 4% low melting agarose and solidified on ice. 200micron thick slices were cut on a Leica VT1200S vibratome and washed and incubated in DMEM/F-12 medium supplemented with 10% fetal bovine serum (FBS) and antibiotics. The PCLS remained viable (MCH-reactive) for at least one week after isolation (data not shown).

Methacholine (MCH) treatment and live imaging

Ex vivo lung slices were experimentally treated with increasing dosages of MCH (acetyl-□-methylchlo-

line chloride, Sigma – A2251), from 100mg/mL to 500mg/mL in HBSS+ solution. MCH is a non-selective muscarinic receptor agonist clinically used to test the severity of asthma in patients. Lungs were incubated in HBSS+ in 24 well plates at 37°C with MCH for 30 minutes, filmed at 30 sec intervals using a Life Technologies EVOS FL Auto microscope to measure bronchoconstriction in response to MCH. In some experiments, 10μM gadolinium (III) chloride hexahydrate (Sigma G7532) and/or 0.8mg/mL albuterol (Sigma PHR1053) were added with MCH 15' after lungs were constricted with 500mg/mL MCH. The ex vivo lung slices were fixed in 4% paraformaldehyde overnight at 4°C before immunostaining.

Immunofluorescence and imaging of fixed PCLS

PFA fixed ex vivo lung slices were incubated for one hour at room temperature in blocking solution: PBS containing 0.1% triton X-100, 0.1% sodium azide, and 2% bovine albumin (BSA) before incubating overnight a 4°C in 1:100 rabbit anti-E-Cadherin (24E10 – Cell Signaling 3195) in blocking solution. Ex vivo lung slices were washed 3 X 30 minutes in PBS before incubating overnight at 4°C overnight with: 1:100 Alexa Fluor 488 goat ant-rabbit IgG (Thermo Scientific - A11008) + 1:250 Alexa Fluor 568 Phalloidin (Thermo Scientific – A12380). Slices were washed 3 X 30 minutes in PBS, stained with 1:1000 DAPI for 20 minutes, mounted, and imaged on a Nikon Eclipse Ti2 spinning disc confocal microscope with a 20X objective.

Live mice MCH challenge with and without treatments

Mice at the end of their immune-priming protocol were placed in a 6.5-quart Hefty® bin that was fitted with an Aerogen® Pro Nebuliser System (AG-AP6000-XX) that produces 2.5-4.0μm volume mean diameter aerosolized particles, adapted from (Bevans et al., 2017). Mice were given two-minute challenges of increasing concentrations of MCH, resting in fresh air for five minutes between challenges, with albuterol (0.8mg/mL) and/or gadolinium (10μM) given in the last three challenges with the highest MCH concentration of 50mg/mL (as outlined in SFig2.). Mice were humanely killed immediately (30' time) or 24hrs post box challenge (-/+ treatments).

Histological analysis and quantification

At the end of their treatments, mice were humanely killed by CO_2 inhalation followed by cervical dislocation. The lungs were inflated by gravity flow with 10% neutral buffered formalin (NBF), excised, and fixed in NBF overnight at room temperature, followed by another overnight room temperature incubation in 70% ethanol. The large lobe was excised and embedded in paraffin. Using a keratome, 3X5μm thick slices were made per slide, 3 slides per lung, each slice made 20μm deeper than the next, and stained with hematoxylin and eosin (H&E) or periodic acid-Schiff (PAS). Histological grades depicted in figures 5 and 6 were used to determine immune cell infiltrate (H&E) and mucous phenotypes (PAS), respectively, with at least five mice analyzed for each group. H&E stained lung slices were also used to determine if the bronchiole epithelium was either damaged or not damaged, with five mice analyzed per group (Fig 4J).

Bronchoalveolar lavage fluid (BALF) isolation and analysis

24 hours after MCH challenge (-/+ treatments), mice were humanely sacrificed, the trachea exposed to make a small incision to accommodate a 20Gx1.25in canula that was secured into place with a nylon suture. 2X1mL of ice-cold PBS was injected into the lungs and ~1.5mL retrieved and analyzed by cytospin and Hema3® staining per manufacture's directions. BALF cells were imaged on a Life Technologies EVOS FL Auto microscope, where eight fields of cells were captured at 40X and the number of eosinophils per field was determined, with at least four mice used for each group.

ELISA and Quantitative Real-time PCR analysis

To confirm the induction of a Th2 inflammatory response from our immune priming protocols, venous IgE levels were determined through blood collection via submandibular vein puncture before and after immune priming and IgE measured by ELISA per manufacturer's instructions (Sigma – RAB0799). The transcript levels of IL-13, IL-4, and Muc5ac (Thermo Fisher TaqMan probes – cat. # 4331182, 4331182, and 4331182, respectively) were measured by quantitative real-time PCR from cDNA transcribed (Thermo Fisher SuperScript™ cat. # - 18091050) from total RNA isolated from whole lung extracts (Qiagen – RNeasy Plus – cat. # 74034) and mRNA expression analysed by a comparative Ct method.

Statistical analysis

To evaluate sample means, we used a non-parametric Mann–Whitney test (Glantz, 2012). To compare more than two groups, we used a Mann–Whitney test with the Holm-Sidak adjustment for pairwise comparisons. For categorical data we used the Chi-Square test to reject the null hypothesis with the Yates correction when analysing two populations and two categories. For analysis of categorical data, when at least 20% of the groups presented frequencies lower than 5 for a given variable, we used the Fisher Exact test.

ACKNOWLEDGEMENTS

We thank the Rama Krishnan and Christopher Reilly labs and Alexandra Locke for help with initial experiments and advice for our paper and Cassandra Deering-Rice for help with RT-PCR. We thank Saranne Mitchell, Carlos Pardo Pastor, Michael Redd, and Teresa Zulueta-Coarasa for helpful comments on our manuscript. An American Asthma Foundation Award 16-0020, National Institute of Health R01GM102169, and a Howard Hughes Faculty Scholar Award 55108560 to J. R., and P30 CA042014 awarded to Huntsman Cancer Institute core and an NCRR Shared Equipment Grant #1S10RR024761-01 for the microscopy core supported this work. We thank the Huntsman Cancer Institute and King's College London Mouse Facilities, the Fluorescence Microscopy Facility at the Health Sciences Cores at the University of Utah, and the Huntsman Cancer Institute Pathology Core, Queen Mary University of London Pathology Core, and the Innovation Hub at King's College London for tissue section handling and scanning.

CONTRIBUTIONS

J. R. designed experiments, interpreted, analyzed data, and wrote the manuscript. D.C.B. and K.F. co-designed experiments, interpreted data, and performed most live and fixed imaging experiments throughout the paper. P. F. R. and M. J. assisted with mouse priming, imaging, and quantification of imaging results of many of the experiments. EOZ provided HDM-primed mice and helped with imaging of ex vivo slices. All authors edited the manuscript.

DECLARATION OF INTERESTS:

The authors declare no competing interests.

REFERENCES

Adams, D.C., Hariri, L.P., Miller, A.J., Wang, Y., Cho, J.L., Villiger, M., Holz, J.A., Szabari, M.V., Hamilos, D.L., Scott Harris, R., et al. (2016). Birefringence microscopy platform for assessing airway smooth muscle structure and function in vivo. Sci Transl Med 8, 359ra131.

Akram, K.M., Yates, L.L., Mongey, R., Rothery, S., Gaboriau, D.C.A., Sanderson, J., Hind, M., Griffiths, M., and Dean, C.H. (2019). Live imaging of alveologenesis in precision-cut lung slices reveals dynamic epithelial cell behaviour. Nature communications 10, 1178-1178.

An, S.S., and Fredberg, J.J. (2007). Biophysical basis for airway hyperresponsiveness. Can J Physiol Pharmacol 85, 700-714.

Andrade, D., and Rosenblatt, J. (2011). Apoptotic regulation of epithelial cellular extrusion. Apoptosis 16, 491-501.

Bae, C., Sachs, F., and Gottlieb, P.A. (2011). The mechanosensitive ion channel Piezo1 is inhibited by the peptide GsMTx4. Biochemistry 50, 6295-6300.

Barbieri, E.J., Bobyock, E., Chernick, W.S., and McMichael, R.F. (1984). The calcium dependency of mucus glycoconjugate secretion by canine tracheal explants. British journal of pharmacology 82, 199-206.

Bendixen, H.H., Smith, G.M., and Mead, J. (1964). Pattern of Ventilation in Young Adults. J Appl Physiol 19, 195-198.

Bevans, T., Deering-Rice, C., Stockmann, C., Rower, J., Sakata, D., and Reilly, C. (2017). Inhaled Remimazolam Potentiates Inhaled Remifentanil in Rodents. Anesth Analg 124, 1484-1490.

Bianchi, A., Dufort, S., Lux, F., Courtois, A., Tillement, O., Coll, J.-L., and Crémillieux, Y. (2014). Quantitative biodistribution and pharmacokinetics of multimodal gadolinium-based nanoparticles for lungs using ultrashort TE MRI. Magnetic Resonance Materials in Physics, Biology and Medicine 27, 303-316.

Castillo, J.R., Peters, S.P., and Busse, W.W. (2017). Asthma Exacerbations: Pathogenesis, Prevention, and Treatment. J Allergy Clin Immunol Pract 5, 918-927.

Davies, D.E. (2009). The role of the epithelium in airway remodeling in asthma. Proc Am Thorac Soc 6, 678-682.

Davis, C.W., and Dickey, B.F. (2008). Regulated Airway Goblet Cell Mucin Secretion. Annual Review of Physiology 70, 487-512.

Deering-Rice, C.E., Shapiro, D., Romero, E.G., Stockmann, C., Bevans, T.S., Phan, Q.M., Stone, B.L., Fassl, B., Nkoy, F., Uchida, D.A., et al. (2015). Activation of TRPA1 by Insoluble Particulate Material and Association with Asthma. Am J Respir Cell Mol Biol.

Deering-Rice, C.E., Stockmann, C., Romero, E.G., Lu, Z., Shapiro, D., Stone, B.L., Fassl, B., Nkoy, F., Uchida, D.A., Ward, R.M., et al. (2016). Characterization of Transient Receptor Potential Vanilloid-1 (TRPV1) Variant Activation by Coal Fly Ash Particles and Associations with Altered Transient Receptor Potential Ankyrin-1 (TRPA1) Expression and Asthma. J Biol Chem 291, 24866-24879.

Deng, X., Zou, W., Xiong, M., Wang, Z., Engelhardt, J.F., Ye, S.Q., Yan, Z., and Qiu, J. (2017). Human Parvovirus Infection of Human Airway Epithelia Induces Pyroptotic Cell Death by Inhibiting Apoptosis. J Virol 91.

Doeing, D.C., and Solway, J. (2013). Airway smooth muscle in the pathophysiology and treatment of asthma. J Appl Physiol (1985) 114, 834-843.

Eisenhoffer, G.T., Loftus, P.D., Yoshigi, M., Otsuna, H., Chien, C.B., Morcos, P.A., and Rosenblatt, J. (2012). Crowding induces live cell extrusion to maintain homeostatic cell numbers in epithelia. Nature 484, 546-549.

Eisenhoffer, G.T., and Rosenblatt, J. (2013). Bringing balance by force: live cell extrusion controls epithelial cell numbers. Trends Cell Biol 23, 185-192.

Goldie, R.G., Fernandes, L.B., Rigby, P.J., and Paterson, J.W. (1988). Epithelial dysfunction and airway hyperreactivity in asthma. Prog Clin Biol Res 263, 317-329.

Golnabi, A.H., Harris, R.S., Venegas, J.G., and Winkler, T. (2014). Deep inspiration and the emergence of ventilation defects during bronchoconstriction: a computational study. PLoS One 9, e112443.

Gu, Y., Forostyan, T., Sabbadini, R., and Rosenblatt, J. (2011). Epithelial cell extrusion requires the sphingosine-1-phosphate receptor 2 pathway. J Cell Biol 193, 667-676.

Gu, Y., and Rosenblatt, J. (2012). New emerging roles for epithelial cell extrusion. Curr Opin Cell Biol 24, 865-870.

Gueders, M.M., Paulissen, G., Crahay, C., Quesada-Calvo, F., Hacha, J., Van Hove, C., Tournoy, K., Louis, R., Foidart, J.M., Noel, A., et al. (2009). Mouse models of asthma: a comparison between C57BL/6 and BALB/c strains regarding bronchial responsiveness, inflammation, and cytokine production. Inflamm Res 58, 845-854.

Hamilton, L.M., Davies, D.E., Wilson, S.J., Kimber, I., Dearman, R.J., and Holgate, S.T. (2001). The bronchial epithelium in asthma--much more than a passive barrier. Monaldi Arch Chest Dis 56, 48-54.

Herrera, A.M., McParland, B.E., Bienkowska, A., Tait, R., Pare, P.D., and Seow, C.Y. (2005). 'Sarcomeres' of smooth muscle: functional characteristics and ultrastructural evidence. J Cell Sci 118, 2381-2392.

Holgate, S.T. (2007). Epithelium dysfunction in asthma. J Allergy Clin Immunol 120, 1233-1244; quiz 1245-1236.

Holgate, S.T. (2011). The sentinel role of the airway epithelium in asthma pathogenesis. Immunol Rev 242, 205-219.

Holgate, S.T., Roberts, G., Arshad, H.S., Howarth, P.H., and Davies, D.E. (2009). The role of the airway epithelium and its interaction with environmental factors in asthma pathogenesis. Proc Am Thorac Soc 6, 655-659.

Holt, P.G., and Sly, P.D. (2012). Viral infections and atopy in asthma pathogenesis: new rationales for asthma prevention and treatment. Nat Med 18, 726-735.

Hopp, R.J., Bewtra, A.K., Nair, N.M., and Townley, R.G. (1984). Specificity and sensitivity of methacholine inhalation challenge in normal and asthmatic children. J Allergy Clin Immunol 74, 154-158.

Krishnan, R., Trepat, X., Nguyen, T.T., Lenormand, G., Oliver, M., and Fredberg, J.J. (2008). Airway smooth muscle and bronchospasm: fluctuating, fluidizing, freezing. Respir Physiol Neurobiol 163, 17-24.

Liesman, R.M., Buchholz, U.J., Luongo, C.L., Yang, L., Proia, A.D., DeVincenzo, J.P., Collins, P.L., and Pickles, R.J. (2014). RSV-encoded NS2 promotes epithelial cell shedding and distal airway obstruction. J Clin Invest 124, 2219-2233.

Lorenzo, I.M., Liedtke, W., Sanderson, M.J., and Valverde, M.A. (2008). TRPV4 channel participates in receptor-operated calcium entry and ciliary beat frequency regulation in mouse airway epithelial cells. Proceedings of the National Academy of Sciences 105, 12611.

Louisias, M., and Phipatanakul, W. (2017). Managing Asthma in Low-Income, Underrepresented Minority, and Other Disadvantaged Pediatric Populations: Closing the Gap. Current allergy and asthma reports 17, 68-68.

Olin, J.T., and Wechsler, M.E. (2014). Asthma: pathogenesis and novel drugs for treatment. BMJ 349,

g5517.

Oyeniran, C., Sturgill, J.L., Hait, N.C., Huang, W.C., Avni, D., Maceyka, M., Newton, J., Allegood, J.C., Montpetit, A., Conrad, D.H., et al. (2015). Aberrant ORM (yeast)-like protein isoform 3 (ORMDL3) expression dysregulates ceramide homeostasis in cells and ceramide exacerbates allergic asthma in mice. J Allergy Clin Immunol 136, 1035-1046 e1036.

Pacheco, C.M., Ciaccio, C.E., Nazir, N., Daley, C.M., DiDonna, A., Choi, W.S., Barnes, C.S., and Rosenwasser, L.J. (2014). Homes of low-income minority families with asthmatic children have increased condition issues. Allergy Asthma Proc 35, 467-474.

Park, H.W., and Tantisira, K.G. (2017). Genetic Signatures of Asthma Exacerbation. Allergy Asthma Immunol Res 9, 191-199.

Persson, C.G. (1996). Epithelial cells: barrier functions and shedding-restitution mechanisms. Am J Respir Crit Care Med 153, S9-10.

Price, M.M., Oskeritzian, C.A., Falanga, Y.T., Harikumar, K.B., Allegood, J.C., Alvarez, S.E., Conrad, D., Ryan, J.J., Milstien, S., and Spiegel, S. (2013). A specific sphingosine kinase 1 inhibitor attenuates airway hyperresponsiveness and inflammation in a mast cell-dependent murine model of allergic asthma. J Allergy Clin Immunol 131, 501-511 e501.

Quantius, J., Schmoldt, C., Vazquez-Armendariz, A.I., Becker, C., El Agha, E., Wilhelm, J., Morty, R.E., Vadasz, I., Mayer, K., Gattenloehner, S., et al. (2016). Influenza Virus Infects Epithelial Stem/Progenitor Cells of the Distal Lung: Impact on Fgfr2b-Driven Epithelial Repair. PLoS Pathog 12, e1005544.

Rogosnitzky, M., and Branch, S. (2016). Gadolinium-based contrast agent toxicity: a review of known and proposed mechanisms. Biometals : an international journal on the role of metal ions in biology, biochemistry, and medicine 29, 365-376.

Rosenblatt, J., Raff, M.C., and Cramer, L.P. (2001). An epithelial cell destined for apoptosis signals its neighbors to extrude it by an actin- and myosin-dependent mechanism. Curr Biol 11, 1847-1857.

Rosner, S.R., Ram-Mohan, S., Paez-Cortez, J.R., Lavoie, T.L., Dowell, M.L., Yuan, L., Ai, X., Fine, A., Aird, W.C., Solway, J., et al. (2014). Airway contractility in the precision-cut lung slice after cryopreservation. Am J Respir Cell Mol Biol 50, 876-881.

Struckmann, N., Schwering, S., Wiegand, S., Gschnell, A., Yamada, M., Kummer, W., Wess, J., and Haberberger, R.V. (2003). Role of muscarinic receptor subtypes in the constriction of peripheral airways: studies on receptor-deficient mice. Mol Pharmacol 64, 1444-1451.

Tam, A., Wadsworth, S., Dorscheid, D., Man, S.F., and Sin, D.D. (2011). The airway epithelium: more than just a structural barrier. Ther Adv Respir Dis 5, 255-273.

Trepat, X., Deng, L., An, S.S., Navajas, D., Tschumperlin, D.J., Gerthoffer, W.T., Butler, J.P., and Fredberg, J.J. (2007). Universal physical responses to stretch in the living cell. Nature 447, 592-595.

Wu, T., Huang, J., Moore, P.J., Little, M.S., Walton, W.G., Fellner, R.C., Alexis, N.E., Peter Di, Y., Redinbo, M.R., Tilley, S.L., et al. (2017). Identification of BPIFA1/SPLUNC1 as an epithelium-derived smooth muscle relaxing factor. Nat Commun 8, 14118.

Xiao, C., Puddicombe, S.M., Field, S., Haywood, J., Broughton-Head, V., Puxeddu, I., Haitchi, H.M., Vernon-Wilson, E., Sammut, D., Bedke, N., et al. (2011). Defective epithelial barrier function in asthma. J Allergy Clin Immunol 128, 549-556 e512.

Yamaya, M. (2012). Virus infection-induced bronchial asthma exacerbation. Pulm Med 2012, 834826.

SUPPLEMENTARY MOVIE LEGENDS

Smovie 1. *Ex vivo* lung slice from an OVA-primed mouse treated with methacholine for 15 minutes. Note high number of extrusions as the bronchiole constricts.

Smovie 2. *Ex vivo* ung slice from an HDM-primed mouse treated with methacholine for 15 minutes. Note high number of extrusions as the bronchiole constricts.

Smovie 3. *Ex vivo* lung slice from an HDM-primed mouse treated with methacholine for 15 minutes, followed by albuterol for 15 minutes. Note high number of extrusions and delamination as the bronchiole constricts, which worsens after the bronchiole relaxes and epithelium pulls away from ASM.

Smovie 4. *Ex vivo* lung slice from an HDM-primed mouse treated with methacholine for 15 minutes followed by albuterol + gadolinium for 15 minutes. Note that epithelial sheet starts to delaminate and then relaxes and attaches back to ASM after addition of albuterol + gadolinium.

Smovie 5. *Ex vivo* lung slice from an non-primed mouse treated with methacholine for 30 minutes does not constrict and there are no extrusions within the airway epithelia.